TSINGHUA SCIENCE AND TECHNOLOGY
ISSN 1007-0214 02/09 pp598-609
Volume 21, Number 6, December 2016

Service-Oriented Wireless Multimedia Multicasting with Partial Frequency Reuse

Quanxin Zhao*, Liang Xu, Yuming Mao, Supeng Leng, Geyong Min, Jia Hu, and Noushin Najjari

Abstract: Service-Oriented Architecture (SOA) is employed in a wide range of applications because it promises to expose computation-intensive tasks as services and combine them with new applications to accelerate their applications development process. For service-oriented multimedia applications, the performance of multicasting transmission services under multimedia traffic must be evaluated. Multiview Video (MVV) is a promising and emerging type of multimedia traffic that consists of multiple video streams, allows stream switching, and requires strict Quality-of-Service (QoS). In this study, we investigated multicast transmission of MVV in wireless cellular networks with Partial Frequency Reuse (PFR) and focused on two challenging problems: (1) multicast group formation and (2) subchannel and power allocation. Initially, we propose a novel Content-based Partial frequency reuse Diversity Grouping (CPDG) scheme to allocate users to multicast groups on the basis of Partial frequency reuse Diversity (PD) in wireless networks with PFR. After group formation, an optimization problem for subchannel and power allocation is formulated to minimize network power consumption under QoS constraint. Thereafter, the optimization problem is divided into two subproblems and solved using simplex method and Karush-Kuhn-Tucker (KKT) condition. Finally, to solve the optimization problem, a suboptimal scheme referred to as Partial frequency reuse Diversity Based Energy-efficient Multicasting (PDEM) is proposed by dynamically allocating wireless resources under QoS constraint. The simulation results show that the proposed PDEM scheme can achieve close-to-optimal performance. Moreover, mathematical analysis of the effect of PD on network performance can provide guidelines for optimization of multimedia traffic in multicasting-enabled wireless cellular networks with PFR.

Key words: service-oriented multimedia; multicast; quality-of-service; frequency reuse diversity

1 Introduction

The emergence of service-oriented communication systems and the rapid growth of multimedia application services[1–3] have led to considerable research attention on multimedia transmission in service-oriented systems. In this study, we focus on traffic transmission for multimedia services, including real-time Ultra High Definition (UHD) video with two types of resolutions (3840×2160 pixels and 7680×4320 pixels), augmented reality, and gaming[4–9], in wireless cellular networks. As a promising and emerging type of multimedia traffic, Multiview Video (MVV) exploits multiple high-definition camera videos to

• Quanxin Zhao, Liang Xu, Yuming Mao, and Supeng Leng are with the School of Communication and Information Engineering, University of Electronic Science and Technology of China, Chengdu 611731, China. E-mail: drqxzhao@gmail.com; xuliang523@hotmail.com; {ymmao, spleng}@uestc.edu.cn.
• Geyong Min, Quanxin Zhao, Jia Hu, and Noushin Najjari are with the College of Engineering, Mathematics and Physical Sciences, University of Exeter, Exeter, EX4 4QF, UK. E-mail: {g.min, q.zhao, j.hu, nn248}@exeter.ac.uk.
∗ To whom correspondence should be addressed.
Manuscript received: 2016-07-12; revised: 2016-09-05; accepted: 2016-10-03

significantly improve picture quality and user Quality-of-Experience (QoE). Such novel multimedia traffic brings great challenges for wireless cellular networks with significantly higher bandwidth requirement than that of existing single camera video.

Most of the existing studies on MVV transmission in wireless cellular networks[5, 10] consider wireless networks with a frequency reuse factor of 1[6, 11, 12], namely, all the cells use the same spectrum. This results in frequent co-channel inter-cell interference on cell edge users, thus rendering user Quality-of-Service (QoS) a great challenge[13, 14]. To eliminate the co-channel inter-cell interference, this study considers wireless networks with Partial Frequency Reuse (PFR), where the frequency resources of a cell are divided by cell center and edge regions, and neighbor cells use orthogonal frequency spectrum in their edge regions.

In multicasting-enabled PFR networks, a group of users requesting the same content have multiple frequency usage policies when they are located in different cell regions. Specifically, cell edge group users can use cell edge resources, while center group users can utilize resources in both the regions. Such multiple frequency usage policies are termed as Partial frequency reuse Diversity (PD). Although multicasting-enabled frequency reuse networks have been investigated in Ref. [15], few studies have focused on the effect of PD on the performance of these networks.

To overcome the abovementioned challenges, we investigate MVV scheduling in multicasting-enabled PFR networks. The primary contributions of this study are summarized below.

- To describe flexible stream switching in MVV and PD, we propose a Content-based Partial frequency reuse Diversity Grouping (CPDG) scheme for allocating network users to multicast groups. Thereafter, some key metrics for PD are proposed on the basis of stream popularity theory to analyze the effect of PD on network performance.
- After allocating network users to multicast groups, an optimization problem is formulated for subchannel and power allocation to minimize system power consumption under user QoS constraint. This optimization problem is then split into two subproblems, and the optimal solutions of these two subproblems are derived using simplex method and Karush-Kuhn-Tucker (KKT) condition, respectively.
- To solve the optimization problem with a low computational complexity, a Partial frequency reuse Diversity based Energy-efficient Multicasting (PDEM) scheme is employed by dynamically allocating wireless resources in different cell regions under user QoS constraint.

The remainder of this paper is organized as follows. Related work is discussed in Section 2. The system model is described in Section 3, and the proposed grouping schemes are presented in Section 4. Section 5 introduces the formulation and analysis of the optimization problem, and Section 6 presents a multicast resource allocation scheme. The obtained simulation results are discussed in Section 7. Finally, conclusions are drawn in Section 8.

2 Related Work

Most studies on video scheduling in wireless networks with frequency reuse have been conducted under unicasting condition[13, 16]. Only a few studies have conducted analysis under multicasting condition. For example, in Ref. [16], adaptive rate scheduling was considered for downlink multicasting of video streams over cellular wireless networks with Fractional Frequency Reuse (FFR) scheduling scheme. Users in the network were classified into different groups according to their experienced Signal-to-Interference-plus-Noise Ratio (SINR) levels. In Ref. [15], mobile users requesting the same content were allocated to a multicast group in multicasting-enabled frequency reuse networks. Thereafter, a low-complexity scheme that maximizes the network Energy Efficiency (EE) under QoS constraint was proposed to allocate frequency resources for both cell edge and center users in the network with FFR scheme. As opposed to existing studies that only focus on wireless resource allocation[15, 16], the current study considers both multicast group formation and wireless resource allocation.

Most of the current studies on transmission of multimedia traffic over wireless cellular networks consider single camera video[16, 17]. Only few studies[5, 6, 15] consider MVV transmission over wireless cellular networks. In Ref. [5], the authors analyzed the path diversity problem for interactive MVV streaming. The system includes a media server that delivers the video to the user over independent network paths. Their proposed proxy can adapt the video transmitted over wireless links in response to channel quality feedback. In Ref. [6], the

authors analyzed stream coding for MVV before its transmission over wireless networks. Subsequently, they proposed a User Dependent Multiview Video Transmission (UDMVT) model to conserve wireless network bandwidth via multicast-unicast-hybrid transmission. Because an MVV consists of multiple video streams, allows stream switching, and requires strict QoS, it brings major challenges for wireless cellular networks in terms of high wireless bandwidth requirement and multiple stream switching. To address these challenges, we employed stream popularity based analysis for flexible stream switching.

In PFR-enabled networks, users in the same multicast group may be at different locations in one cell, e.g., some users may be located in the cell center region, while others may be located in the edge region. This results in different frequency usage policies for users in the same group. Namely, users located in the edge region can use the edge frequency spectrum, whereas users located at the center can use both center and edge spectra, which are referred to as PD. In Ref. [17], the authors employed soft frequency reuse in single-frequency networks under enhanced Multimedia Broadcast Multicast Service (eMBMS) to improve eMBMS coverage of high data rates and cell-edge throughput of broadcast services. When compared with previous studies on traffic scheduling in multicasting-enabled PFR networks[15–17], this study is the first to address the PD problem and analyze its effect on system performance.

3 System Model

We consider an Orthogonal Frequency Division Multiple Access (OFDMA) based base station with partial frequency reuse. Let us consider an MVV with C camera streams, where the camera stream set is denoted as $\mathcal{C}=\{c, c=1,2,\ldots,C\}$. Zipf distribution based stream popularity is used[18, 19], where the probability for playing the c-th most popular stream is calculated as $p_c=(1/c^s)/\sum_{i=1}^{C}(1/i^s)$, where $0\leqslant p_c\leqslant 1, \sum_c p_c=1$. Further, s is the parameter for Zipf distribution.

The whole frequency band in the PFR network is divided by $\mathcal{F}=\cup_{i=0}^{3}\mathcal{F}_i$, where $\mathcal{F}_i\cap\mathcal{F}_j=\varnothing, i\neq j, i, j\in\{0,1,2,3\}$[15]. The cell edge band is $\mathcal{F}_i$ $(i=1,2,3)$, and the cell center band is $\mathcal{F}_0$. Further, $\mathcal{M}$ is the subchannel set, where the cardinality of $\mathcal{M}$, $|\mathcal{M}|$, denotes the total number of subchannels.

Let i $(i\in\mathcal{M}^{\mathrm{I}})$ and o $(o\in\mathcal{M}^{\mathrm{O}})$ denote cell center and edge subchannels, respectively, where $\mathcal{M}^{\mathrm{I}}\cup\mathcal{M}^{\mathrm{O}}=\mathcal{M}$. Moreover, $\gamma_{k,g,c}$ is content request indicator, i.e., user k at location g requesting stream $c\in\mathcal{C}$, where $k\in\mathcal{K}=\{1,2,\ldots,K\}$, and g is the geographic location for cell center area $g\in G^{\mathrm{I}}$ and cell edge area $g\in G^{\mathrm{O}}$. Other mathematical symbols are listed in Table 1.

The equivalent channel gain of a geographic area g playing stream c on a subchannel is the worst channel gain user in that group as given below.

$$\begin{cases}|h_{g,c,o}|^2=\min\limits_{k\in\mathcal{K}_{g,c}}\{|h_{k,o}|^2\},\forall g\in\mathcal{G}^{\mathrm{O}},\text{cell edge};\\ |h_{g,c,i}|^2=\min\limits_{k\in\mathcal{K}_{g,c}}\{|h_{k,i}|^2\},\forall g\in\mathcal{G}^{\mathrm{I}},\text{cell center}\end{cases}\tag{1}$$

System power consumption is the total power of all the allocated subchannels in both regions as follows:

$$\begin{cases}P_{\mathrm{tot}}=P_{\mathrm{tot}}^{\mathrm{O}}(\boldsymbol{\rho}^{\mathbf{O}},\boldsymbol{p}^{\mathbf{O}})+P_{\mathrm{tot}}^{\mathrm{I}}(\boldsymbol{\rho}^{\mathbf{I}},\boldsymbol{p}^{\mathbf{I}}),\\ P_{\mathrm{tot}}^{\mathrm{O}}(\boldsymbol{\rho}^{\mathbf{O}},\boldsymbol{p}^{\mathbf{O}})=\sum\limits_{o\in\mathcal{M}^{\mathrm{O}}}\left(p_o\left(\sum\limits_{g\in\mathcal{G}^{\mathrm{O}}}\sum\limits_{c\in\mathcal{C}}\rho_{g,c,o}\right)\right),\\ P_{\mathrm{tot}}^{\mathrm{I}}(\boldsymbol{\rho}^{\mathbf{I}},\boldsymbol{p}^{\mathbf{I}})=\sum\limits_{i\in\mathcal{M}^{\mathrm{I}}}\left(p_i\left(\sum\limits_{g\in\mathcal{G}^{\mathrm{I}}}\sum\limits_{c\in\mathcal{C}}\rho_{g,c,i}\right)\right)\end{cases}\tag{2}$$

where $\boldsymbol{p}^{\mathbf{O}}=[p_o]_{1\times|\mathcal{M}^{\mathrm{O}}|}$ and $\boldsymbol{p}^{\mathbf{I}}=[p_i]_{1\times|\mathcal{M}^{\mathrm{I}}|}$ are cell edge and center power allocation vectors, respectively.

System throughput is the summation data rate of all the users as follows:

$$\begin{cases}R_{\mathrm{tot}}=R_{\mathrm{tot}}^{\mathrm{O}}(\boldsymbol{\rho}^{\mathbf{O}},\boldsymbol{p}^{\mathbf{O}})+R_{\mathrm{tot}}^{\mathrm{I}}(\boldsymbol{\rho}^{\mathbf{I}},\boldsymbol{p}^{\mathbf{I}}),\\ R_{\mathrm{tot}}^{\mathrm{O}}(\boldsymbol{\rho}^{\mathbf{O}},\boldsymbol{p}^{\mathbf{O}})=\sum\limits_{o\in\mathcal{M}^{\mathrm{O}}}\sum\limits_{g\in\mathcal{G}^{\mathrm{O}}}\sum\limits_{c\in\mathcal{C}}\rho_{g,c,o}R_{g,c,o}=\\ \sum\limits_{o\in\mathcal{M}^{\mathrm{O}}}\sum\limits_{g\in\mathcal{G}^{\mathrm{O}}}\sum\limits_{c\in\mathcal{C}}\rho_{g,c,o}|\mathcal{K}_{g,c}|B_0\log_2\left(1+\frac{p_o|h_{g,c,o}|^2}{N_0B_0}\right),\\ R_{\mathrm{tot}}^{\mathrm{I}}(\boldsymbol{\rho}^{\mathbf{I}},\boldsymbol{p}^{\mathbf{I}})=\sum\limits_{i\in\mathcal{M}^{\mathrm{I}}}\sum\limits_{g\in\mathcal{G}^{\mathrm{I}}}\sum\limits_{c\in\mathcal{C}}\rho_{g,c,i}R_{g,c,i}=\end{cases}$$

Table 1 Main mathematical symbols.

Symbol	Meaning
g,k,c	Index of geographic area, user, and stream
$\mathcal{G}^{\mathrm{I}},\mathcal{G}^{\mathrm{O}}$	Index set of center and edge groups
i,o	Index of available cell center and edge subchannel
$\mathcal{M}^{\mathrm{I}}$	Index set of available cell center subchannels
$\mathcal{M}^{\mathrm{O}}$	Index set of available cell edge subchannels
$\mathcal{M}$	Index set of the total system available subchannels
ξ	Division factor of the total system subchannels
$P_{\max}$	Maximum transmitted power of base station
B	Total system bandwidth

$$\sum_{i\in\mathcal{M}^{\mathrm{I}}}\sum_{g\in\mathcal{G}^{\mathrm{I}}}\sum_{c\in\mathcal{C}}\rho_{g,c,i}|\mathcal{K}_{g,c}|B_0\log_2\left(1+\frac{p_i|h_{g,c,i}|^2}{N_0B_0}\right) \tag{3}$$

If subchannel x is allocated to stream c in geographic area g, then $\rho_{g,c,x}=1$. Otherwise, $\rho_{g,c,x}=0$. $R_{g,c,x}$ is the summation data rate of all the users in $|\mathcal{K}_{g,c}|$ playing stream c in geographic area g on subchannel x. Further, p_o and p_i are the power values of cell edge subchannel o and cell center subchannel i, respectively. Moreover, we define $\boldsymbol{\rho}^{\mathbf{O}}=[\rho_{g,c,o}]_{|\mathcal{G}^{\mathrm{O}}|\times|\mathcal{C}^{\mathrm{O}}|\times|\mathcal{M}^{\mathrm{O}}|}$ and $\boldsymbol{\rho}^{\mathbf{I}}=[\rho_{g,c,i}]_{|\mathcal{G}^{\mathrm{I}}|\times|\mathcal{C}^{\mathrm{I}}|\times|\mathcal{M}^{\mathrm{I}}|}$ as the subchannel allocation indicator matrix. Let N_0 and $B_0=B/|\mathcal{M}|$ denote the power spectral density of additive white Gaussian noise and bandwidth of a subchannel, respectively.

4 Partial Frequency Reuse Diversity Based User Grouping

A user grouping scheme referred to as CPDG scheme that is based on PD for multicasting-enabled PFR networks is proposed. Subsequently, some key metrics for PD users are proposed for analyzing the effect of PD on the network.

The CPDG scheme, shown in Algorithm 1, is described in detail below. In the case of an MVV, the CPDG scheme operates iteratively for each stream. In each iteration, the CPDG scheme first selects the most popular stream. Thereafter, users requesting the above chosen stream are allocated to different cell region sets $\mathcal{U}_c$ and $\mathcal{V}_c$. Two types of multicast groups are then formed: (1) conventional groups for cell center and edge are derived as $\mathcal{Q}_c^1$ and $\mathcal{Q}_c^2$ by allocating PD users in the center region. (2) If there exists at least one user in both cell center and edge regions, $\mathcal{Q}_c^3$ and $\mathcal{Q}_c^4$ are obtained respectively for cell center and edge by allocating PD users in the center region. Finally, the CPDG outputs two types of groups including the conventional case in $\mathcal{Q}_c^1$ and $\mathcal{Q}_c^2$, and PD-enabled case in $\mathcal{Q}_c^3$ and $\mathcal{Q}_c^4$. After obtaining the multicast groups under PD-enabled and conventional cases, the system can decide which type of group must be used before resource allocation.

Next, some key metrics such as probability and number of PD users are proposed for PD users on the basis of stream popularity.

Definition 1 The probabilities of at least one PD user for the c-th most popular stream and for all C streams, respectively, are given as

Algorithm 1 Content based PFR Diversity Grouping Scheme

Require:
Content request : $\gamma_{k,g,c}$
User set : $\mathcal{K}$
Cell center user set for stream c: $\mathcal{U}_c$
Cell edge user set for stream c: $\mathcal{V}_c$
Request probability of stream c: p_c
Conventional set of groups of stream c: $\mathcal{Q}_c^1, \mathcal{Q}_c^2$
PD enabled set of groups of stream c: $\mathcal{Q}_c^3, \mathcal{Q}_c^4$

Ensure:
for stream $c=\arg\max_{c\in\mathcal{C}}(p_c)$ **do**
  for user $k\in\mathcal{K}$ **do**
    if $(\gamma_{k,g,c}==1)\&\&(g\in\mathcal{G}^{\mathrm{O}})$ **then**
      $\mathcal{V}_c\leftarrow k$
      $\mathcal{K}=\mathcal{K}\setminus k$
    else if $(\gamma_{k,g,c}==1)\&\&(g\in\mathcal{G}^{\mathrm{I}})$ **then**
      $\mathcal{U}_c\leftarrow k$
      $\mathcal{K}=\mathcal{K}\setminus k$
    end if
  end for
  $\mathcal{Q}_c^1\Leftarrow\mathcal{U}_c$
  $\mathcal{Q}_c^2\Leftarrow\mathcal{V}_c$
  if $\mathcal{U}_c\neq\varnothing$ && $\mathcal{V}_c\neq\varnothing$ **then**
    $\mathcal{Q}_c^3\Leftarrow\mathcal{U}_c$
    $\mathcal{Q}_c^4\Leftarrow\mathcal{U}_c\cup\mathcal{V}_c$
  end if
end for
Output: $\mathcal{Q}_c^1, \mathcal{Q}_c^2; \mathcal{Q}_c^3, \mathcal{Q}_c^4$.

$$\mathrm{PPD}_c=(1-(1-p_c)^U)(1-(1-p_c)^V) \tag{4}$$

$$\mathrm{PPD}=1-\prod_{c=1}^{C}(1-\mathrm{PPD}_c) \tag{5}$$

where U and V are the number of cell center and cell edge users, respectively.

Definition 2 The average number of PD users for the c-th most popular stream and all C streams, respectively, are as follows:

$$\mathrm{NPD}_c=Up_c(1-(1-p_c)^V) \tag{6}$$

$$\mathrm{NPD}=\sum_{c=1}^{C}\mathrm{NPD}_c \tag{7}$$

5 Optimization Problem and Analysis

In this section, we introduce an optimization problem to minimize power consumption of multicasting-enabled PFR networks under user QoS constraint. The optimization problem can be expressed as follows:

$$\mathbf{P0:}\ \min_{\substack{\boldsymbol{\rho}^{\mathbf{O}},\boldsymbol{\rho}^{\mathbf{I}}\\ \boldsymbol{p}^{\mathbf{O}},\boldsymbol{p}^{\mathbf{I}}}} P_{\mathrm{tot}}=P_{\mathrm{tot}}^{\mathrm{O}}(\boldsymbol{\rho}^{\mathbf{O}},\boldsymbol{p}^{\mathbf{O}})+P_{\mathrm{tot}}^{\mathrm{I}}(\boldsymbol{\rho}^{\mathbf{I}},\boldsymbol{p}^{\mathbf{I}}) \tag{8}$$

subject to

$$\begin{cases}
\text{C1: } (1-t_{g,c})C_{g,c} \leqslant \dfrac{\sum\limits_{o\in\mathcal{M}^{\mathrm{O}}}\rho_{g,c,o}R_{g,c,o}}{|\mathcal{K}_{g,c}|}, \forall g\in\mathcal{G}^{\mathrm{O}};\\
\text{C2: } (1-t_{g,c})C_{g,c} \leqslant \dfrac{\sum\limits_{i\in\mathcal{M}^{\mathrm{I}}}\rho_{g,c,i}R_{g,c,i}}{|\mathcal{K}_{g,c}|}, \forall g\in\mathcal{G}^{\mathrm{I}};\\
\text{C3: } \sum\limits_{g\in\mathcal{G}^{\mathrm{O}}}\sum\limits_{c\in\mathcal{C}}\rho_{g,c,o}\leqslant 1, \forall o\in\mathcal{M}^{\mathrm{O}};\\
\text{C4: } \sum\limits_{g\in\mathcal{G}^{\mathrm{I}}}\sum\limits_{c\in\mathcal{C}}\rho_{g,c,i}\leqslant 1, \forall i\in\mathcal{M}^{\mathrm{I}};\\
\text{C5: } \rho_{\mathrm{go,co},o}+\rho_{\mathrm{gi,ci},i}\leqslant 1, \forall o\in\mathcal{M}^{\mathrm{O}}, i\in\mathcal{M}^{\mathrm{I}},\\
\quad \forall \mathrm{go}\in\mathcal{G}^{\mathrm{O}}, \mathrm{gi}\in\mathcal{G}^{\mathrm{I}}, \mathrm{co}\in\mathcal{C}_{\mathrm{go}}, \mathrm{ci}\in\mathcal{C}_{\mathrm{gi}};\\
\text{C6: } \sum\limits_{o\in\mathcal{M}^{\mathrm{O}}}\sum\limits_{g\in\mathcal{G}^{\mathrm{O}}}\sum\limits_{c\in\mathcal{C}}\rho_{g,c,o}\leqslant \dfrac{1}{\eta}\cdot(1-\xi)\cdot|\mathcal{M}|;\\
\text{C7: } \sum\limits_{i\in\mathcal{M}^{\mathrm{I}}}\sum\limits_{g\in\mathcal{G}^{\mathrm{I}}}\sum\limits_{c\in\mathcal{C}}\rho_{g,c,i}\leqslant \xi\cdot|\mathcal{M}|;\\
\text{C8: } \sum\limits_{o\in\mathcal{M}^{\mathrm{O}}}p_o+\sum\limits_{i\in\mathcal{M}^{\mathrm{I}}}p_i\leqslant P_{\max};\\
\text{C9: } \rho_{g,c,o}\in\{0,1\}, \forall o\in\mathcal{M}^{\mathrm{O}}, \forall g\in\mathcal{G}^{\mathrm{O}}, c\in\mathcal{C};\\
\text{C10: } \rho_{g,c,i}\in\{0,1\}, \forall i\in\mathcal{M}^{\mathrm{I}}, \forall g\in\mathcal{G}^{\mathrm{I}}, c\in\mathcal{C};\\
\text{C11: } 0\leqslant p_o\leqslant P_{\max}, \forall o\in\mathcal{M}^{\mathrm{O}};\\
\text{C12: } 0\leqslant p_i\leqslant P_{\max}, \forall i\in\mathcal{M}^{\mathrm{I}}
\end{cases}$$

where constant $C_{g,c}$ is the average data rate, i.e., QoS requirement for users playing stream c in geographic area g. Further, $t_{g,c}\in\mathcal{T}=\{\alpha,\beta\}$, ($\alpha\in[0,1]$ and $\beta\in[0,1]$) are system parameters for cell edge and cell center data rate requirements, respectively. Because the streams are distinct, no more than one stream can be simultaneously allocated on a subchannel, as given in Constraints 3 and 4.

The NP-hard optimization problem **P0** has two independent variables, $\boldsymbol{\rho}$ and $\boldsymbol{p}$; hence, the optimal results cannot be easily obtained. Therefore, we convert **P0** into two sub-optimal problems, **P1** and **P2**. First, **P1** is introduced to allocate subchannels with equal power level for all subchannels. This is a mixed integer programming problem, and it will be converted into a linear programming problem via constraints zooming. Second, on the basis of results of **P1**, **P2** allocates the optimal power to sub-channels, thus resulting in a concave programming problem.

$$\mathbf{P1:}\ \min_{\boldsymbol{\rho}^{\mathbf{O}},\,\boldsymbol{\rho}^{\mathbf{I}}} P_{\mathrm{tot}}=P_{\mathrm{tot}}^{\mathrm{O}}(\boldsymbol{\rho}^{\mathbf{O}})+P_{\mathrm{tot}}^{\mathrm{I}}(\boldsymbol{\rho}^{\mathbf{I}}) \tag{9}$$

subject to

$$\begin{cases}
\text{C1, C2, C3, C4, C5, C6, C7;}\\
\text{C9}^*: 0\leqslant\rho_{g,c,o}\leqslant 1, \forall o\in\mathcal{M}^{\mathrm{O}}, \forall g\in\mathcal{G}^{\mathrm{O}}, c\in\mathcal{C};\\
\text{C10}^*: 0\leqslant\rho_{g,c,i}\leqslant 1, \forall i\in\mathcal{M}^{\mathrm{I}}, \forall g\in\mathcal{G}^{\mathrm{I}}, c\in\mathcal{C}
\end{cases}$$

$$\mathbf{P2:}\ \min_{\boldsymbol{p}^{\mathbf{O}},\,\boldsymbol{p}^{\mathbf{I}}} P_{\mathrm{tot}}=P_{\mathrm{tot}}^{\mathrm{O}}(\boldsymbol{p}^{\mathbf{O}})+P_{\mathrm{tot}}^{\mathrm{I}}(\boldsymbol{p}^{\mathbf{I}}) \tag{10}$$

subject to C1, C2, C8, C11, C12

Lemma 1 For a given resource allocation matrix $[\boldsymbol{\rho}^{\mathbf{O}},\boldsymbol{\rho}^{\mathbf{I}}]$, the primary problem **P0** is transformed into problem **P2**, which is a convex programming problem with optimal solution expressed as

$$\begin{cases}
\widetilde{p}_o=\left[L_o-\dfrac{\sum\limits_{g\in\mathcal{G}^{\mathrm{O}}}\sum\limits_{c\in\mathcal{C}}\frac{N_0B_0}{|h_{g,c,o}|^2}}{\sum\limits_{g\in\mathcal{G}^{\mathrm{O}}}\sum\limits_{c\in\mathcal{C}}1}\right]_0^{P_{\max}}, \forall o\in\mathcal{M}^{\mathrm{O}};\\
\widetilde{p}_i=\left[L_i-\dfrac{\sum\limits_{g\in\mathcal{G}^{\mathrm{I}}}\sum\limits_{c\in\mathcal{C}}\frac{N_0B_0}{|h_{g,c,i}|^2}}{\sum\limits_{g\in\mathcal{G}^{\mathrm{I}}}\sum\limits_{c\in\mathcal{C}}1}\right]_0^{P_{\max}}, \forall i\in\mathcal{M}^{\mathrm{I}}
\end{cases} \tag{11}$$

where $[x]_a^b$ represents the Euclidean projection of x on $[a,b]$. The tags of L_o and L_i are introduced to satisfy the following formula:

$$\begin{aligned}
L_o&=\frac{\ln 2B_0\sum\limits_{g\in\mathcal{G}^{\mathrm{O}}}\sum\limits_{c\in\mathcal{C}}\widetilde{u}_{g,c}^{\mathrm{O}}\cdot\rho_{g,c,o}}{\left(\sum\limits_{g\in\mathcal{G}^{\mathrm{O}}}\sum\limits_{c\in\mathcal{C}}1\right)\cdot\left(\sum\limits_{g\in\mathcal{G}^{\mathrm{O}}}\sum\limits_{c\in\mathcal{C}}\rho_{g,c,o}+w\right)}\\
L_i&=\frac{\ln 2B_0\sum\limits_{g\in\mathcal{G}^{\mathrm{I}}}\sum\limits_{c\in\mathcal{C}}\widetilde{u}_{g,c}^{\mathrm{I}}\cdot\rho_{g,c,i}}{\left(\sum\limits_{g\in\mathcal{G}^{\mathrm{I}}}\sum\limits_{c\in\mathcal{C}}1\right)\cdot\left(\sum\limits_{g\in\mathcal{G}^{\mathrm{I}}}\sum\limits_{c\in\mathcal{C}}\rho_{g,c,i}+w\right)}
\end{aligned} \tag{12}$$

where $\widetilde{u}_{g,c}^{\mathrm{O}}$, $\widetilde{u}_{g,c}^{\mathrm{I}}$, and w are Lagrangian multipliers. See Appendix for details of Lemma 1.

If a feasible solution exists for **P1**, it is then determined by $C_{g,c}$. In order to conveniently determine the feasibility of the above problem, we establish the following model:

$$\mathbf{P3.1}: \max_{\boldsymbol{\rho}^{\mathbf{O}}} C_{g,c}^{\mathrm{O}}=\frac{\sum\limits_{o\in\mathcal{M}^{\mathrm{O}}}\rho_{g,c,o}B_0\log_2\left(1+\frac{p_o|h_{g,c,o}|^2}{N_0B_0}\right)}{|\mathcal{K}_{g,c}|} \tag{13}$$

subject to

$$\begin{cases}
\text{C3}: \sum\limits_{g\in\mathcal{G}^{\mathrm{O}}}\sum\limits_{c\in\mathcal{C}}\rho_{g,c,o}\leqslant 1, \forall o\in\mathcal{M}^{\mathrm{O}};\\
\text{C5.1}^*: 0\leqslant\rho_{g,c,o}\leqslant(1-\chi), \forall o\in\mathcal{M}^{\mathrm{O}}, \forall g\in\mathcal{G}^{\mathrm{O}}
\end{cases}$$

$$\mathbf{P3.2}: \max_{\boldsymbol{\rho}^{\mathbf{I}}} C_{g,c}^{\mathrm{I}}=\frac{\sum\limits_{i\in\mathcal{M}^{\mathrm{I}}}\rho_{g,c,i}B_0\log_2\left(1+\frac{p_i|h_{g,c,i}|^2}{N_0B_0}\right)}{|\mathcal{K}_{g,c}|} \tag{14}$$

subject to

$$\begin{cases} \text{C4}: \sum\limits_{g\in\mathcal{G}^{\text{I}}}\sum\limits_{c\in\mathcal{C}}\rho_{g,c,i}\leqslant 1, \forall i\in\mathcal{M}^{\text{I}}; \\ \text{C5.2}^*: \ 0\leqslant\rho_{g,c,i}\leqslant\chi, \forall i\in\mathcal{M}^{\text{I}}, \forall g\in\mathcal{G}^{\text{I}}, c\in\mathcal{C} \end{cases}$$

where χ represents the parameter restricting the scope of the decision variables to meet the Constraint 5 in **P1**. The optimal solutions of **P3.1** and **P3.2** can help determine if the inequality relations in Constraints 1 and 2 are true, respectively, which are necessary conditions for that **P1** has a feasible solution.

6 Resource Allocation Algorithm

To solve the optimization problem with a low computational complexity, we introduce PDEM scheme to dynamically allocate wireless resources under user QoS constraint, as discussed below.

For the first step of the PDEM scheme, shown in Algorithm 2, cell edge subchannel allocation is employed. A pair of $[g,c]$ achieving the lowest data rate is then selected. Thereafter, cell edge subchannel o^* achieving the maximum data rate is allocated to the chosen pair $[g,c]$. Finally, the available cell edge subchannel set and data rate are updated. The iteration will stop if the QoS requirements of all the users are satisfied. For the second step, cell center subchannel allocation is applied, which follows a process similar to that of the first step. After obtaining the subchannel allocation results under equal power assumption for all subchannels, the optimal power is calculated using Eq. (11) and reallocated to subchannels.

Complexity analysis: In Algorithm 2, the iterations of the first while loop (Lines 1–16) are limited by the scale of the cell edge subchannel set and cell edge geographic stream set. Two extreme cases are considered below. In the first case, the system has limited frequency resources where all the cell edge subchannels cannot satisfy the QoS requirements of all the cell edge groups. In the second case, the system has sufficient frequency resources where any cell edge subchannel can satisfy the QoS requirements of all the cell edge groups. In the first case, a subchannel is deleted (Line 11) after allocation, thus resulting in at most $|\mathcal{M}^{\text{O}}|$ iterations. In the latter case, a pair of cell edge geographic streams is removed (Line 14) after satisfying the QoS constraint, thus leading to at most $|\mathcal{O}_{g,c}|$ iterations. Moreover, the first for loop (Lines 6–8) results in $|\mathcal{M}^{\text{O}}|$ iterations. Because cell center subchannel allocation (Lines 17–32) is similar to cell edge subchannel allocation, the computational complexity

Algorithm 2 Partial Frequency Reuse Diversity based Energy-Efficient Multicasting

Require:
Required data rate of stream-c in area-g: $C_{g,c}$
Achieved data rate of stream-c in area-g: $r_{g,c}$
Cell edge geographic stream set: $\mathcal{O}_{g,c}$
Cell center geographic stream set: $\mathcal{I}_{g,c}$
Available cell edge subchannels index set: $\mathcal{M}^{\text{O}}$
Available cell center subchannels index set: $\mathcal{M}^{\text{I}}$

Ensure:

1: **while** $(O_{g,c}\neq\varnothing)$ && $(\mathcal{M}^{\text{O}}\neq\varnothing)$ **do**
2: Find $[g^*,c^*]\Leftarrow\arg\min\limits_{g\in\mathcal{G}^{\text{O}}}\left\{\min\limits_{c\in\mathcal{C}}\frac{r_{g,c}}{(1-t_{g,c})C_{g,c}}\right\}$.
3: **if** $1\leqslant\frac{r_{g^*,c^*}}{(1-t_{g^*,c^*})C_{g^*,c^*}}$ **then**
4: Jump out of the **while-loop**
5: **end if**
6: **for** each $o\in\mathcal{M}^{\text{O}}$ **do**
7: Calculate $R_{g^*,c^*,o}$ by Eq. (3)
8: **end for**
9: Find $[o^*]\Leftarrow\arg\max\limits_{o\in\mathcal{M}^{\text{O}}}\{R_{g^*,c^*,o}\}$.
10: Allocate o^* to $[g^*,c^*]$.
11: Update $\mathcal{M}^{\text{O}}\Leftarrow\mathcal{M}^{\text{O}}\setminus o^*$.
12: Update $r_{g^*,c^*}\Leftarrow r_{g^*,c^*}+R_{g^*,c^*,o^*}$.
13: **if** $1\leqslant\frac{r_{g^*,c^*}}{(1-t_{g^*,c^*})C_{g^*,c^*}}$ **then**
14: Delete pair $O_{g,c}=O_{g,c}\setminus[g^*,c^*]$
15: **end if**
16: **end while**
17: **while** $(I_{g,c}\neq\varnothing)$ && $(\mathcal{M}^{\text{I}}\neq\varnothing)$ **do**
18: Find $[g^*,c^*]\Leftarrow\arg\min\limits_{g\in\mathcal{G}^{\text{I}}}\left\{\min\limits_{c\in\mathcal{C}}\frac{r_{g,c}}{(1-t_{g,c})C_{g,c}}\right\}$.
19: **if** $1\leqslant\frac{r_{g^*,c^*}}{(1-t_{g^*,c^*})C_{g^*,c^*}}$ **then**
20: Jump out of the **while-loop**
21: **end if**
22: **for** each $i\in\mathcal{M}^{\text{I}}$ **do**
23: Calculate $R_{g^*,c^*,i}$ by Eq. (3)
24: **end for**
25: Find $[i^*]\Leftarrow\arg\max\limits_{i\in\mathcal{M}^{\text{I}}}\{R_{g^*,c^*,i}\}$.
26: Allocate i^* to $[g^*,c^*]$.
27: Update $\mathcal{M}^{\text{I}}\Leftarrow\mathcal{M}^{\text{I}}\setminus i^*$.
28: Update $r_{g^*,c^*}\Leftarrow r_{g^*,c^*}+R_{g^*,c^*,i^*}$.
29: **if** $1\leqslant\frac{r_{g^*,c^*}}{(1-t_{g^*,c^*})C_{g^*,c^*}}$ **then**
30: Delete pair $I_{g,c}=I_{g,c}\setminus[g^*,c^*]$
31: **end if**
32: **end while**

of PDEM is $O(|\mathcal{M}^{\text{O}}||L^{\text{O}}|+|\mathcal{M}^{\text{I}}||\mathcal{L}^{\text{I}}|)$, where $|\mathcal{L}^{\text{O}}|=\max(|\mathcal{M}^{\text{O}}|,|\mathcal{O}_{g,c}|)$ and $|\mathcal{L}^{\text{I}}|=\max(|\mathcal{M}^{\text{I}}|,|\mathcal{I}_{g,c}|)$ denote the maximum number of iterations in the two extreme cases.

7 Performance Evaluation

The performance of multicasting-enabled PFR network with MVV is simulated to investigate multicast group

formation and wireless resource allocation. First, the multicast group formation scheme CPDG and PD are investigated from three perspectives: the probability of at least one PD user, the average number of PD users, and the average number of groups. Second, the proposed PDEM scheme is compared with the optimal solution to analyze its performance in terms of throughput, power consumption, and energy efficiency.

In the MVV, different numbers of users and cameras are considered. Further, PFR(x/y) denotes the cell center occupying x subchannels over y total subchannels. Three schemes OPT, ReOPT, and PDEM are compared. Specifically, OPT stands for the optimal solution of **P1** solved by CVX[20]. Because the value of subchannel allocation indicator ρ solved by OPT can be decimal, a suboptimal scheme ReOPT is proposed to obtain integer subchannel allocation results for a real network by rounding the value of ρ calculated from OPT to an integer 0 or 1. The subchannel and power allocation processes operate iteratively in OPT and ReOPT schemes. Therefore, another suboptimal scheme PDEM is used to eliminate iterations and reduce computational complexity when compared with the OPT and ReOPT schemes.

Figure 1 shows the requesting probability for each stream under different Zipf distribution parameters. Eight camera streams are present in the MVV. Streams 1 and 8 are the most and the least popular streams. Namely, the larger the stream ID, the less popular the stream. In Fig. 1, an increasing gap in requesting probability can be seen between the most and the least popular streams as the value of s increases. Therefore, as the value of s increases, the requesting probability is higher for playing more popular streams.

Figure 2 shows the probability that there exists at least one PD user requesting the c-th popular stream, i.e., PPD_c. For different values of parameter s, the number of cell center users U and number of cell edge users V are considered. For the same number of users, an increasing gap of probability exists between the most and the least popular streams as the value of s increases. This is in accordance with the results of Fig. 1. Moreover, the probability for each stream under ($U = 15, V = 15$) is higher than that under ($U = 5$, $V = 25$), thus indicating that the closer the number of center and edge users, the higher the probability of at least one PD user for each stream.

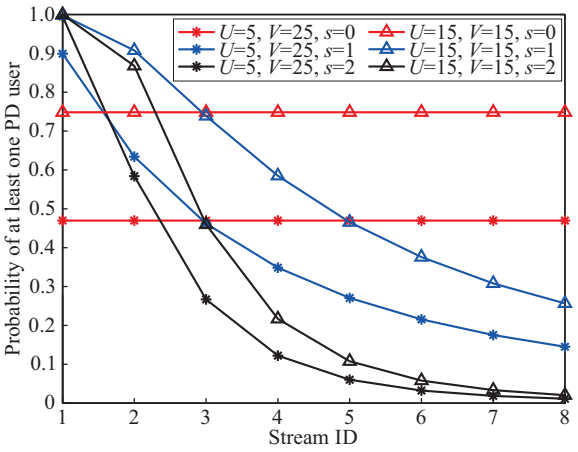

Fig. 2 Probability of at least one PD user versus stream ID.

Figure 3 shows the average number of PD users for each stream, i.e., NPD_c. Different Zipf parameters s and three cases of user distributions ($U = 5, V = 25$), ($U = 15, V = 15$), and ($U = 25, V = 5$) are considered. The increase in the number of center users U results in a larger gap between the number of users of the most and the least popular streams. Moreover, the difference in number of users between the most and the least popular streams increases as the value of s

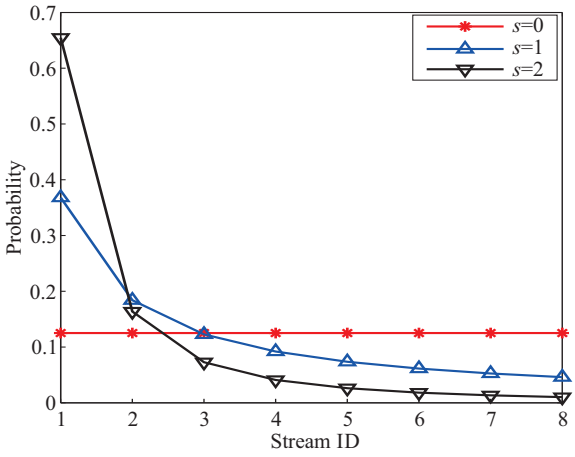

Fig. 1 Request probability for each stream.

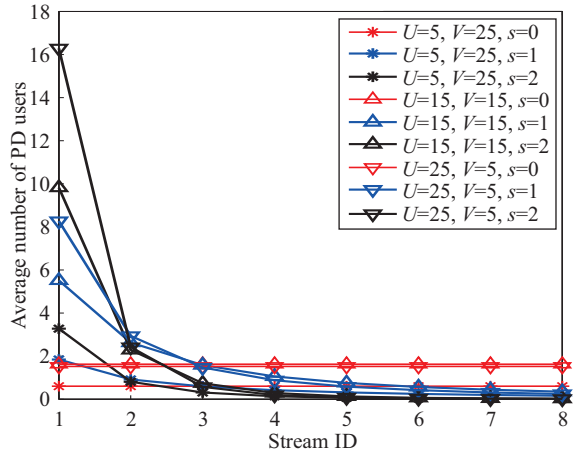

Fig. 3 Average number of PD users versus stream ID.

increases.

Figure 4 shows the variation in average number of PD users NPD_c versus the number of cameras. Eight MVVs are considered, and each MVV has 1–8 cameras. The results show that the number of PD users increases as the number of center users U increases. Moreover, significant difference can be seen between the number of users in cases of 1 camera and 8 cameras, with more center users.

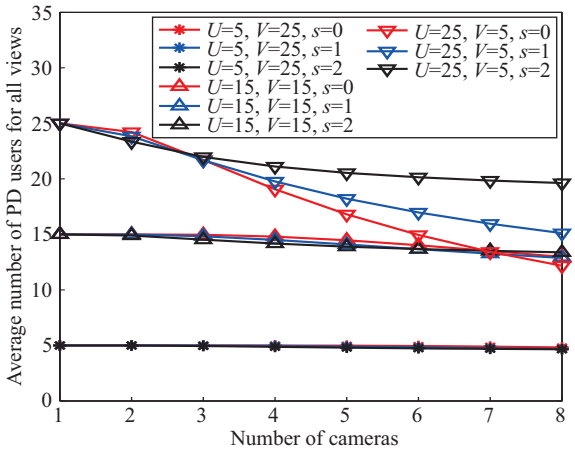

Fig. 4 Average number of PD users for all views.

Figures 5 and 6 show the variation in total number of center and edge groups with number of cameras. Eight MVVs are considered, and each MVV has 1–8 cameras. Different values of parameter s and three cases of user distributions $(U = 5, V = 25)$, $(U = 15, V = 15)$, and $(U = 25, V = 5)$ are considered. As can be seen in Fig. 5, the number of center groups increases as the value of s decreases. Moreover, the number of center groups increases as the number of center users increases. Figure 6 shows that when the PD users are served by cell edge, the number of edge groups increases as the value of s decreases. Moreover, the smaller the number of center users, the larger the number of edge groups.

Figure 7 shows the variation in throughput, transmit

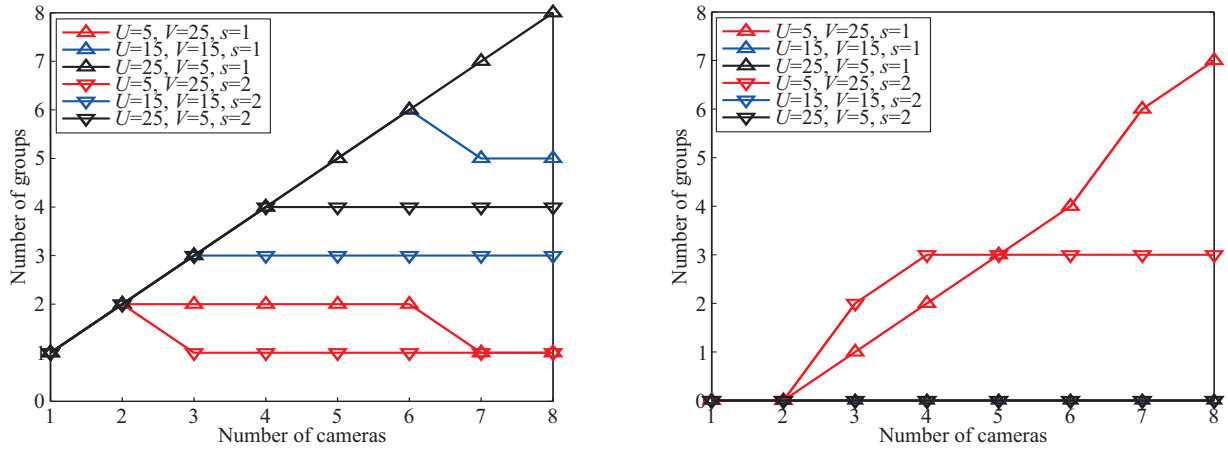

(a) Center (b) Edge

Fig. 5 Number of groups versus number of cameras with cell center served PD users.

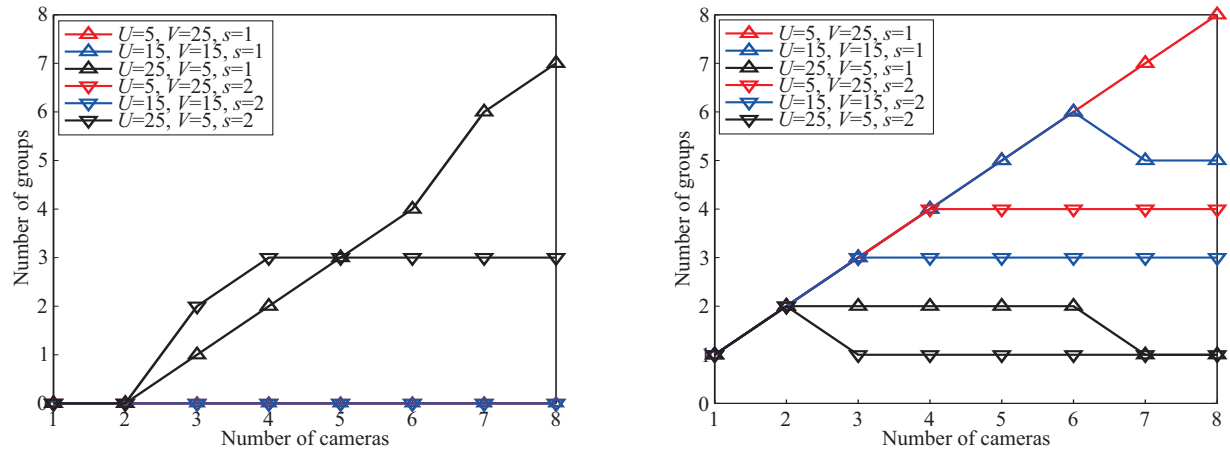

(a) Center (b) Edge

Fig. 6 Number of groups versus number of cameras with cell edge served PD users.

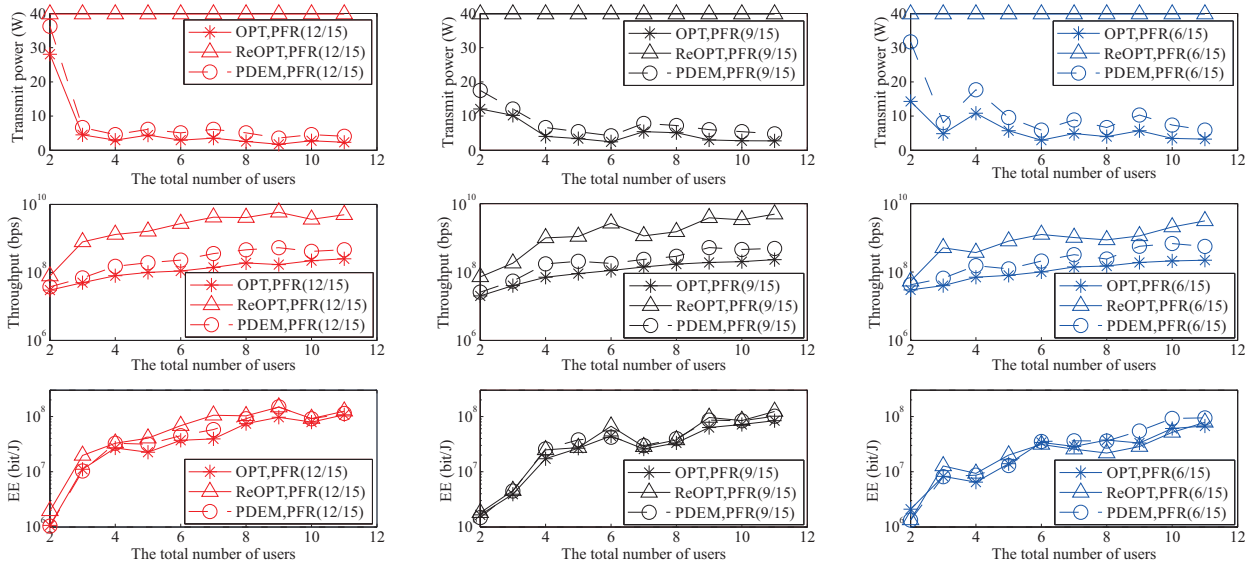

Fig. 7 Throughput, power, and energy efficiency against various numbers of users.

power, and Energy Efficiency (EE) with total number of users for the three schemes. Different frequency usage policies PFR (x/y) are considered. The results show that when the system power consumption is optimized, the transmit power of PDEM scheme is similar to that of the optimal scheme OPT. Moreover, the throughput of the PDEM scheme is lower than that of the ReOPT scheme but higher than that of OPT scheme. Therefore, the proposed PDEM scheme achieves close-to-optimal performance.

Figure 8 shows the variation in performance of the PDEM scheme in terms of throughput, transmit power, and EE with number of groups under different frequency usage policies PFR (x/y) and numbers of users K. The transmit power results show that as the number of groups increases, the transmit power gradually increases to the maximum value. Thereafter, the throughput decreases as the number of groups increases because the maximum power is shared by increasing number of groups. Therefore, the throughput of each group will decrease as a result of smaller allocated power. Moreover, as the number of users increases, the number of users in each group increases, thus resulting in enhanced throughput.

8 Conclusion

In this study, we analyzed service-oriented multimedia traffic scheduling in wireless cellular networks with

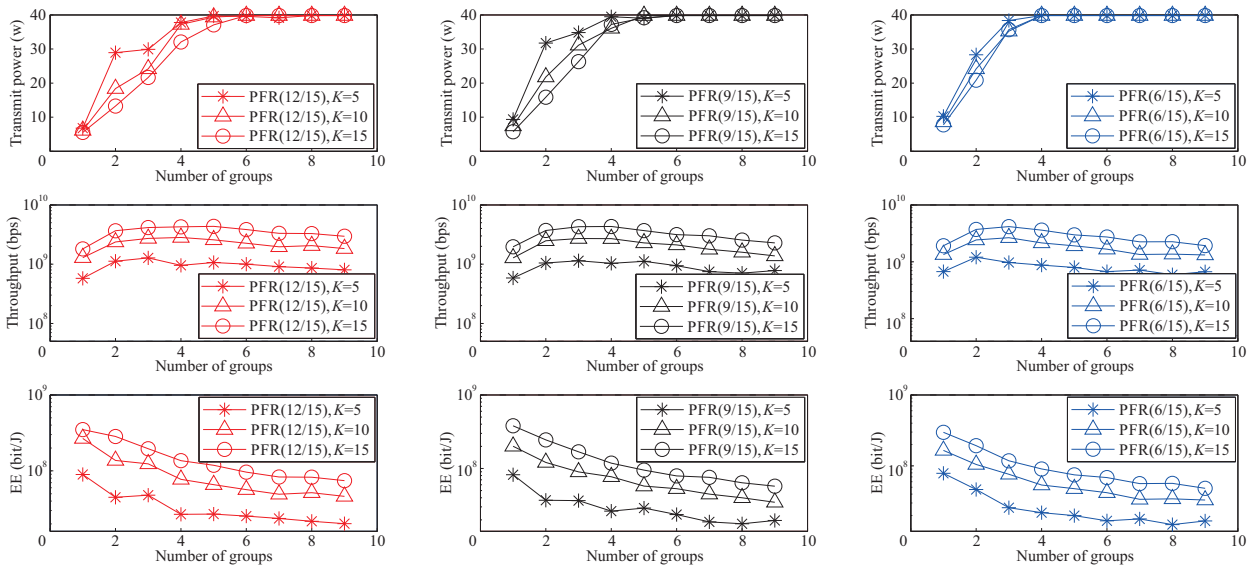

Fig. 8 Throughput, power, and energy efficiency for different number of groups.

PFR. First, to allocate users to multicast groups, a CPDG scheme was proposed using PD. Subsequently, we formulated an optimization problem for wireless resources allocation with the aim of minimizing network power consumption under QoS constraint, which was then relaxed to two suboptimal problems and solved using Lagrangian function. Thereafter, to solve the optimization problem with reduced computational complexity, a PDEM scheme was proposed by dynamically allocating wireless resources in PFR-enabled networks. The simulation results show that the number of cameras in an MVV influences the number of PD users. Further, the numbers of groups in different cell regions are related to both Zipf distribution parameters and the cell regions of PD users. Moreover, the proposed PDEM scheme can achieve a close-to-optimal performance.

Appendix

Proof Problem **P2** is equivalent to problem **P2*** through deformation of equation.

$$\mathbf{P2}^*: \min_{\boldsymbol{p}^{\mathrm{O}},\,\boldsymbol{p}^{\mathrm{I}}} P_{\mathrm{tot}} = P_{\mathrm{tot}}^{\mathrm{O}}(\boldsymbol{p}^{\mathbf{O}}) + P_{\mathrm{tot}}^{\mathrm{I}}(\boldsymbol{p}^{\mathbf{I}}) \tag{15}$$

subject to

$$\begin{cases} C1^*: L_{g,c}^{\mathrm{O}} \leqslant 0, \forall g \in \mathcal{G}^{\mathrm{O}}, c \in \mathcal{C}; \\ C2^*: L_{g,c}^{\mathrm{I}} \leqslant 0, \forall g \in \mathcal{G}^{\mathrm{I}}, c \in \mathcal{C}; \\ C8: L^P \leqslant 0; \\ C11: 0 \leqslant p_o \leqslant P_{\max}, \forall o \in \mathcal{M}^{\mathrm{O}}; \\ C12: 0 \leqslant p_i \leqslant P_{\max}, \forall i \in \mathcal{M}^{\mathrm{I}}; \end{cases}$$

where we define the following tags:

$$\begin{aligned} L_{g,c}^{\mathrm{O}} &= (1 - t_{g,c}) C_{g,c} |\mathcal{K}_{g,c}| \\ &\quad - \sum_{o \in \mathcal{M}^{\mathrm{O}}} \rho_{g,c,o} B_0 \log_2 \left(1 + \frac{p_o |h_{g,c,o}|^2}{N_0 B_0}\right), \\ L_{g,c}^{\mathrm{I}} &= \left(1 - t_{g,c}\right) C_{g,c} |\mathcal{K}_{g,c}| \\ &\quad - \sum_{i \in \mathcal{M}^{\mathrm{I}}} \rho_{g,c,i} B_0 \log_2 \left(1 + \frac{p_i |h_{g,c,i}|^2}{N_0 B_0}\right), \\ L^P &= \sum_{o \in \mathcal{M}^{\mathrm{O}}} p_o + \sum_{i \in \mathcal{M}^{\mathrm{I}}} p_i - P_{\max}. \end{aligned}$$

Let us consider that the objective function and all the above tag functions in problem **P2*** are convex functions. We can then conclude that the equivalent problem **P2** is a convex programming problem.

On the basis of the above fact, we can use KKT conditions to solve problem **P2*** to obtain the optimization solution. First, we define the Lagrangian function $L : \mathbb{R}^{|\mathcal{M}^{\mathrm{O}}+\mathcal{M}^{\mathrm{I}}|} \to \mathbb{R}$ associated with problem **P2** as follows:

$$\begin{aligned} L([\boldsymbol{p}^{\mathrm{O}}, \boldsymbol{p}^{\mathrm{I}}], [\boldsymbol{u}^{\mathrm{O}}, \boldsymbol{u}^{\mathrm{I}}], w) &= P_{\mathrm{tot}}^{\mathrm{O}}(\boldsymbol{p}^{\mathbf{O}}) + P_{\mathrm{tot}}^{\mathrm{I}}(\boldsymbol{p}^{\mathbf{I}}) - \\ \sum_{g \in \mathcal{G}^{\mathrm{O}}} \sum_{c \in \mathcal{C}} u_{g,c}^{\mathrm{O}} L_{g,c}^{\mathrm{O}} &- \sum_{g \in \mathcal{G}^{\mathrm{I}}} \sum_{c \in \mathcal{C}} u_{g,c}^{\mathrm{I}} L_{g,c}^{\mathrm{I}} + w \cdot L^P \end{aligned} \tag{16}$$

where $u_{g,c}^{\mathrm{O}}$, $u_{g,c}^{\mathrm{I}}$, and w are Lagrangian multipliers. Particularly, we define $\boldsymbol{u}^{\mathrm{O}} = [u_{g,c}^{\mathrm{O}}]_{|\mathcal{G}^{\mathrm{O}}| \times |\mathcal{C}^{\mathrm{O}}|}$ and $\boldsymbol{u}^{\mathrm{I}} = [u_{g,c}^{\mathrm{I}}]_{|\mathcal{G}^{\mathrm{I}}| \times |\mathcal{C}^{\mathrm{I}}|}$ as the Lagrangian multiplier matrix. For $\forall o \in \mathcal{M}^{\mathrm{O}}$ and $\forall i \in \mathcal{M}^{\mathrm{I}}$, we obtain

$$\begin{cases} \frac{\partial L}{\partial p_o} = \sum\limits_{g \in \mathcal{G}^{\mathrm{O}}} \sum\limits_{c \in \mathcal{C}} \rho_{g,c,o} - \\ \qquad \sum\limits_{g \in \mathcal{G}^{\mathrm{O}}} \sum\limits_{c \in \mathcal{C}} \widetilde{u}_{g,c}^{\mathrm{O}} \dfrac{\rho_{g,c,o} B_0 \cdot \ln 2}{\widetilde{p}_o + \frac{N_0 B_0}{|h_{g,c,o}|^2}} + w, \\ \frac{\partial L}{\partial p_i} = \sum\limits_{g \in \mathcal{G}^{\mathrm{I}}} \sum\limits_{c \in \mathcal{C}} \rho_{g,c,i} - \\ \qquad \sum\limits_{g \in \mathcal{G}^{\mathrm{I}}} \sum\limits_{c \in \mathcal{C}} \widetilde{u}_{g,c}^{\mathrm{I}} \dfrac{\rho_{g,c,i} B_0 \cdot \ln 2}{\widetilde{p}_i + \frac{N_0 B_0}{|h_{g,c,i}|^2}} + w \end{cases} \tag{17}$$

Let $\partial L / \partial p_o = 0$ and $\partial L / \partial p_i = 0$, then

$$\begin{cases} \sum\limits_{g \in \mathcal{G}^{\mathrm{O}}} \sum\limits_{c \in \mathcal{C}} \widetilde{u}_{g,c}^{\mathrm{O}} \dfrac{\rho_{g,c,o} B_0 \cdot \ln 2}{\widetilde{p}_o + \frac{N_0 B_0}{|h_{g,c,o}|^2}} = \sum\limits_{g \in \mathcal{G}^{\mathrm{O}}} \sum\limits_{c \in \mathcal{C}} \rho_{g,c,o} + w, \\ \sum\limits_{g \in \mathcal{G}^{\mathrm{I}}} \sum\limits_{c \in \mathcal{C}} \widetilde{u}_{g,c}^{\mathrm{I}} \dfrac{\rho_{g,c,i} B_0 \cdot \ln 2}{\widetilde{p}_i + \frac{N_0 B_0}{|h_{g,c,i}|^2}} = \sum\limits_{g \in \mathcal{G}^{\mathrm{I}}} \sum\limits_{c \in \mathcal{C}} \rho_{g,c,i} + w \end{cases} \tag{18}$$

For the sake of simplicity, we can assume that

$$\begin{cases} \sum\limits_{g \in \mathcal{G}^{\mathrm{O}}} \sum\limits_{c \in \mathcal{C}} \widetilde{u}_{g,c}^{\mathrm{O}} \dfrac{\rho_{g,c,o} B_0 \cdot \ln 2}{\widetilde{p}_o + \frac{N_0 B_0}{|h_{g,c,o}|^2}} \approx \dfrac{\sum\limits_{g \in \mathcal{G}^{\mathrm{O}}} \sum\limits_{c \in \mathcal{C}} \widetilde{u}_{g,c}^{\mathrm{O}} \rho_{g,c,o} B_0 \cdot \ln 2}{\sum\limits_{g \in \mathcal{G}^{\mathrm{O}}} \sum\limits_{c \in \mathcal{C}} \left(\widetilde{p}_o + \dfrac{N_0 B_0}{|h_{g,c,o}|^2}\right)}, \\ \sum\limits_{g \in \mathcal{G}^{\mathrm{I}}} \sum\limits_{c \in \mathcal{C}} \widetilde{u}_{g,c}^{\mathrm{I}} \dfrac{\rho_{g,c,i} B_0 \cdot \ln 2}{\widetilde{p}_i + \frac{N_0 B_0}{|h_{g,c,i}|^2}} \approx \dfrac{\sum\limits_{g \in \mathcal{G}^{\mathrm{I}}} \sum\limits_{c \in \mathcal{C}} \widetilde{u}_{g,c}^{\mathrm{I}} \rho_{g,c,i} B_0 \cdot \ln 2}{\sum\limits_{g \in \mathcal{G}^{\mathrm{I}}} \sum\limits_{c \in \mathcal{C}} \left(\widetilde{p}_i + \dfrac{N_0 B_0}{|h_{g,c,i}|^2}\right)} \end{cases} \tag{19}$$

According to Eq. (19), Eq. (18) can be revised as follows:

$$\begin{cases} \dfrac{\ln 2 B_0 \sum\limits_{g \in \mathcal{G}^{\mathrm{O}}} \sum\limits_{c \in \mathcal{C}} \widetilde{u}_{g,c}^{\mathrm{O}} \cdot \rho_{g,c,o}}{\sum\limits_{g \in \mathcal{G}^{\mathrm{O}}} \sum\limits_{c \in \mathcal{C}} \left(\widetilde{p}_o + \dfrac{N_0 B_0}{|h_{g,c,o}|^2}\right)} = \sum\limits_{g \in \mathcal{G}^{\mathrm{O}}} \sum\limits_{c \in \mathcal{C}} \rho_{g,c,o} + w, \\ \dfrac{\ln 2 B_0 \sum\limits_{g \in \mathcal{G}^{\mathrm{I}}} \sum\limits_{c \in \mathcal{C}} \widetilde{u}_{g,c}^{\mathrm{I}} \cdot \rho_{g,c,i}}{\sum\limits_{g \in \mathcal{G}^{\mathrm{I}}} \sum\limits_{c \in \mathcal{C}} \left(\widetilde{p}_i + \dfrac{N_0 B_0}{|h_{g,c,i}|^2}\right)} = \sum\limits_{g \in \mathcal{G}^{\mathrm{I}}} \sum\limits_{c \in \mathcal{C}} \rho_{g,c,i} + w \end{cases} \tag{20}$$

Through deformation of Eq. (20), Lemma 1 is proved to be true. ■

Acknowledgment

This work was supported by the EU FP7 Project CLIMBER (PIRSES-GA-2012-318939), the program of China Scholarship Council (No. 201506070027), and National Key Technology Research and Development Program of China (No. 2015BAH08F01).

References

[1] Y. Zhang, G. Cui, Y. Wang, X. Guo, and S. Zhao, An optimization algorithm for service composition based on an improved FOA, *Tsinghua Sci. Technol.,* vol. 20, no. 1, pp. 90–99, 2015.

[2] C. Xiang, P. Yang, X. Wu, H. He, and S. Xiao, QoS-based service selection with lightweight description for large-scale service-oriented internet of things, *Tsinghua Sci. Technol.,* vol. 20, no. 4, pp. 336–347, 2015.

[3] S. Zeng, S. Huang, and Y. Fan, Service-oriented enterprise network performance analysis, *Tsinghua Sci. Technol.,* vol. 14, no. 4, pp. 492–503, 2009.

[4] M. K. Kang, D. Y. Kim, and K. J. Yoon, Adaptive support of spatial-temporal neighbors for depth map sequence up-sampling, *IEEE Signal Process. Lett.,* vol. 21, no. 2, pp. 150–154, 2014.

[5] J. Chakareski, Wireless streaming of interactive multi-view video via network compression and path diversity, *IEEE Trans. on Commun.,* vol. 62, no. 4, pp. 1350–1357, 2014.

[6] T. Fujihashi, Z. Pan, and T. Watanabe, UMSM: A traffic reduction method on multi-view video streaming for multiple users, *IEEE Trans. on Multimedia,* vol. 16, no. 1, pp. 228–241, 2014.

[7] D. A. Abreu, P. Frossard, and F. Pereira, Optimizing multiview video plus depth prediction structures for interactive multiview video streaming, *IEEE J. Sel. Top. Signal Process.,* vol. 9, no. 3, pp. 487–500, 2015.

[8] Y. Ye, Y. He, and X. Xiu, Manipulating ultra-high definition video traffic, *IEEE Multimedia,* vol. 22, no. 3, pp. 73–81, 2015.

[9] M. K. Seo, S. H. Baek, and K. H. Park, Arrangement of multi-dimensional scalable video data for heterogeneous clients, *Inf. Syst.*, vol. 35, no. 2, pp. 237–259, 2009.

[10] H. S. Park and S. B. Cho, A personalized summarization of video life-logs from an indoor multi-camera system using a fuzzy rule-based system with domain knowledge, *Inf. Syst.,* vol. 36, no. 8, pp. 1124–1134, 2011.

[11] B. W. Micallef, C. J. Debono, and R. A. Farrugia, Low complexity disparity estimation for immersive 3D video transmission, presented at IEEE International Conference on Communications Workshops, Budapest, Hungary, 2013.

[12] H. Seo and K. Lee, Effective scalable video streaming transmission with TBS algorithm in an MC-CDMA system, *Inf. Syst.,* vol. 48, no. 1, pp. 313–319, 2015.

[13] O. G. Aliu, M. Mehta, M. Imran, A. Karandikar, and B. Evans, A new cellular-automata-based fractional frequency reuse scheme, *IEEE Trans. on Vehicular Technol.,* vol. 64, no. 4, pp. 1535–1547, 2014.

[14] M. Qian, W. Hardjawana, Y. Li, B. Vucetic, X. Yang, and J. Shi, Adaptive soft frequency reuse scheme for wireless cellular networks, *IEEE Trans. on Vehicular Technol.,* vol. 64, no. 1, pp. 118–131, 2015.

[15] Q. Zhao, Y. Mao, S. Leng, and G. Min, QoS-aware energy-efficient multicast for multi-view video with fractional frequency reuse, presented at the 10th EAI International Conference on Communications and Networking in China, Shanghai, China, 2015.

[16] H. B. Chang, I. Rubine, and O. Hadar, Scalable video downlink multicasting in multi-cell cellular wireless networks, presented at IEEE Globecom Workshops, Austin, USA, 2014.

[17] C. Reis, A. Correia, N. Souto, and M. M. D. Silva, On enhanced multimedia broadcast multicast service for 4G, presented at the 21st International Conference on Telecommunications, Lisbon, Portugal, 2014.

[18] D. Ren, S. H. G. Chan, G. Cheung, and P. Frossard, Coding structure and replication optimization for interactive multiview video streaming, *IEEE Trans. on Multimedia,* vol. 16, no. 7, pp. 1874–1887, 2014.

[19] Z. Chen, L. Sun, and S. Yang, Overcoming view switching dynamic in multi-view video streaming over P2P network, presented at 3DTV-Conference: The True Vision-Capture, Transmission and Display of 3D Video, Tampere, Finland, 2010.

[20] M. Grant and S. Boyd, CVX: Matlab software for disciplined convex programming, http://cvxr.com/cvx, 2015.

Quanxin Zhao received the BS degree from Zhengzhou University in 2010. He is currently a PhD candidate in the School of Communication & Information Engineering, University of Electronic Science and Technology of China (UESTC). His research focuses on resource, spectrum, energy and networking in wireless networks, broadband wireless access networks, and the next generation mobile networks.

Liang Xu received the BS degree from University of Electronic Science and Technology of China in 2012. He is currently pursuing the PhD degree in communication engineering at University of Electronic Science and Technology of China. His research interests include radio resource management, heterogeneous networks, ultra-dense networks, game theory, and machine learning in 5G networks.

Geyong Min is a professor of high performance computing and networking at the Department of Mathematics and Computer Science University of Exeter, United Kingdom. He received the PhD degree in computing science from the University of Glasgow, United Kingdom, in 2003, and the BSc degree from Huazhong University of Science and Technology, China, in 1995. His research interests include future internet, computer networks, wireless communications, multimedia systems, information security, high performance computing, ubiquitous computing, modelling and performance engineering.

Jia Hu received the PhD degree in computer science from the University of Bradford, UK, in 2010, and MEng and BEng degrees in physical electronics and communications engineering from Huazhong University of Science and Technology, Wuhan, China, in 2006 and 2004, respectively. He is a lecturer in computer science at the University of Exeter. He has published over 40 research papers in prestigious international journals and at reputable international conferences. His research interests include performance evaluation, next generation networking, resource allocation and optimization, energy-efficiency, network security, smart city, and big data.

Noushin Najjari is a PhD student at the Department of Computer Science, University of Exeter, UK. She received the MSc degree in information technology from Sharif University of Technology, Iran, in 2010, and the BSc degree from Alzahra University, Iran, in 2006. Her research interests include performance modelling and analysis of communication networks, next generation networking, wireless network protocols, energy-efficiency, and cross-layer optimization.

Yuming Mao is a professor with University of Electronic Science and Technology of China. He is the Chairman of the Department of Network Engineering. He received the MS degree in communication and information engineering from University of Electronic Science and Technology of China in 1984. His main research area includes broadband communication network, network organization and protocol analysis, TCP/IP technology, network management and protocol, routing protocol, and network engineering. He was recipient of several awards, including the first grade, second grade, and third grade awards of the Ministry of Electronic Industry for science and technology progress, the second grade National Award for science and technology progress.

Supeng Leng received the PhD degree from Nanyang Technological University (NTU), Singapore in 2005. He is a professor with the School of Communication and Information Engineering, University of Electronic Science and Technology of China, Chengdu, China. He was a research fellow with the Network Technology Research Center, NTU from 2004 to 2005. He has published over 100 research papers. His research interests include resource, spectrum, energy, routing, and networking in broadband wireless access networks, vehicular networks, Internet of Things, next-generation mobile networks, and smart grids. He served as an Organizing Committee Chair and a Technical Program Committee Member for many international conferences, and a Reviewer for over ten international research journals.